Forming Planets in Magnetized Accretion Disks

UPPSALA UNIVERSITET

W. LYRA[1], A. JOHANSEN[2], H. KLAHR[2] & N. PISKUNOV[1]

1. Uppsala Astronomical Observatory, Box 515, 751 20, Uppsala, Sweden
2. Max-Planck-Institut für Astronomie, Königstuhl 17, 69117 Heidelberg, Germany

Abstract

We present global 3D MHD simulations of disks of gas and solids, developing models that can be used to study various scenarios of planet formation in turbulent accretion disks. We employ the PENCIL CODE, a high-order finite-difference particle-mesh code using Cartesian coordinates. These "disk-in-a-box" models sustain MHD turbulence, in good agreement with published results achieved with cylindrical codes. We investigate the dependence of the magnetorotational instability on disk scale height, finding evidence that the resulting turbulent stresses depend on temperature. We also study the dynamics of solids in the hydromagnetic turbulence. The vertical turbulent diffusion of the embedded boulders is comparable to the turbulent viscosity of the flow. Significant overdensities arise in the solid component as boulders concentrate in high pressure regions.

Problem Setup

We model the turbulent disks as specified below:

- Cartesian uniform grid centered in the star.
- Physical Domain : Radius(s) = 0.4 - 2.5, L_z = 0.5
- Cylindrical gravitational potential $\Phi = GM/s$
- Locally isothermal equation of state : $T = c_{s_0}^2/s^{q_T}$
- Resolution x, y, z=320x320xN_z
- Hyper (6[th] order) and Shock-Capturing Dissipation
- Simulation over 100 dynamical times

The conversion to physical units is provided below.

Table 1. Conversion between code and physical units

Quantity	Physical unit
Length	5.2 AU
Density	2.0×10^{-11} g cm^{-3}
Velocity	13.06 km s^{-1}
Energy	1.60×10^{43} ergs
Pressure, Stress	34 dyne cm^{-2}
Time	1.89 yr
Magnetic Field	20.71 G
Viscosity	1.02×10^{20} cm^2 s^{-1}

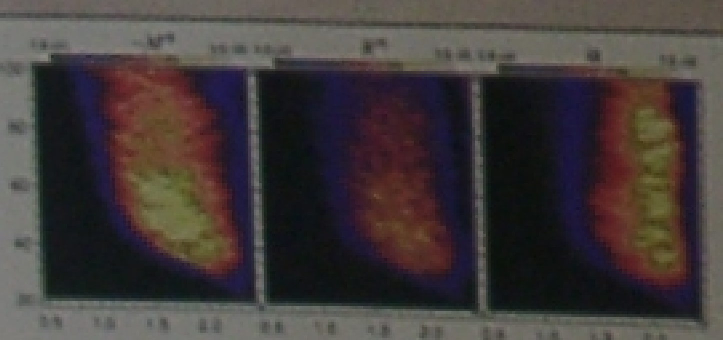

Spacetime diagram of the turbulent stresses and alpha viscosity for model F. Time is quoted in orbits at s_0=1.0. Saturation is reached at 40 orbits, but after 60 orbits the stresses seem to start a slow decay. The alpha viscosity appears constant, due to a similar decay in gas pressure in the outer disk, that starts to deplete as the resulting accretion builds a negative density gradient.

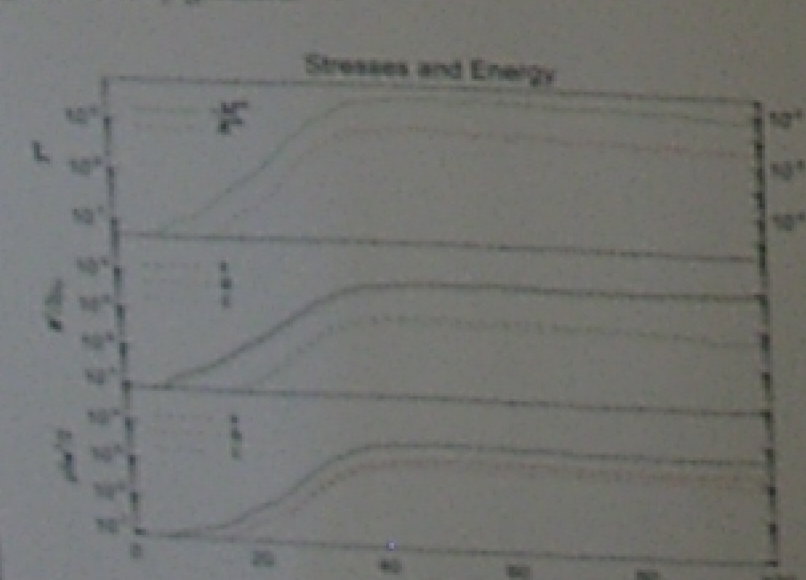

Time evolution of the turbulence for model F. The top panel shows the evolution of the $r\phi$-component of the Maxwell and Reynolds stresses, while the middle and bottom panels show the evolution of magnetic and kinetic energy, respectively. The solid line indicates the total energy. The toroidal field dominates the magnetic energy, as the Keplerian motion drags the frozen-in field lines.

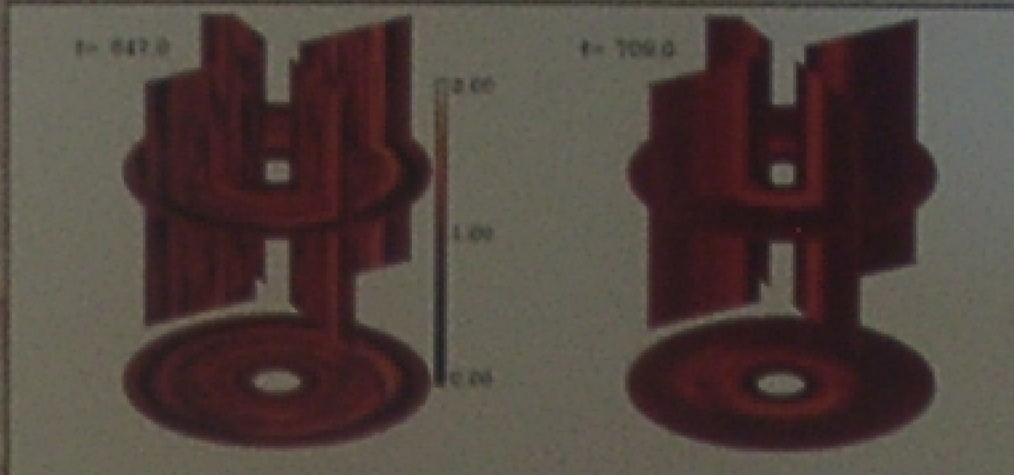

Density contours at selected planes z=0, y=0, and x=0 on saturated turbulent state for sound speed profiles of c_{s_0} = 0.05 (model A, left panel) and c_{s_0} = 0.20 (model C, right panel). The stronger stresses for the hotter case lead to a much more effective turbulent viscosity, as seen from the steep density profile resulting from accretion. The vertical planes are stretched to show more detail than the correct aspect ratio would allow.

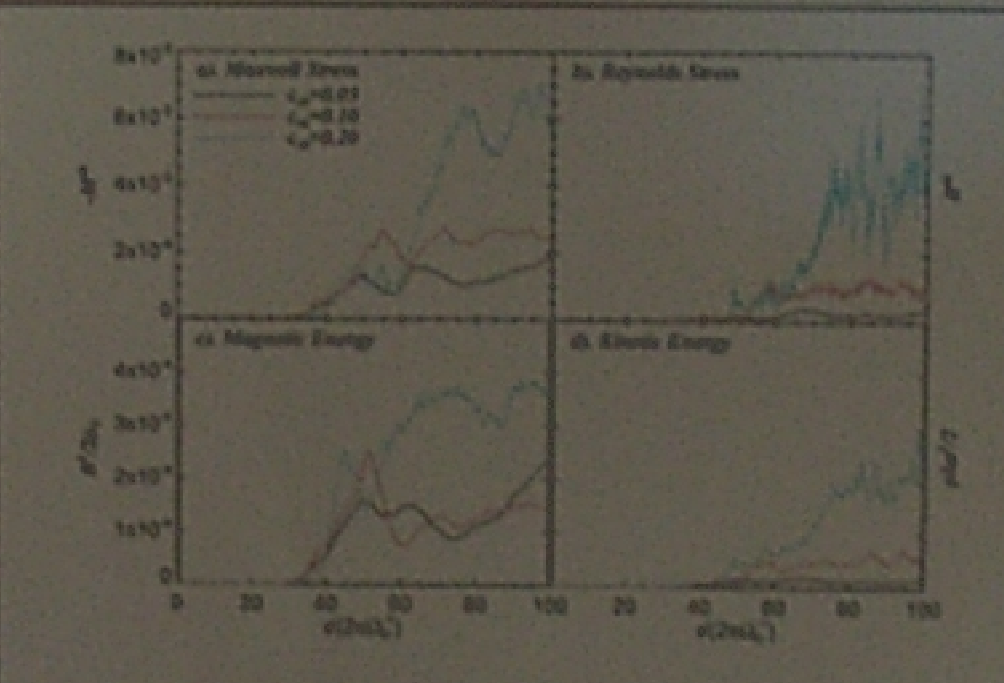

Time evolution of the turbulence for different sound speed profiles (models A, B and C). The strength of the angular momentum transport differs with sound speed. The increase in stress observed when the sound speed is raised to c_{s_0} =0.20 is dramatic. Time is quoted in orbits at s_0.

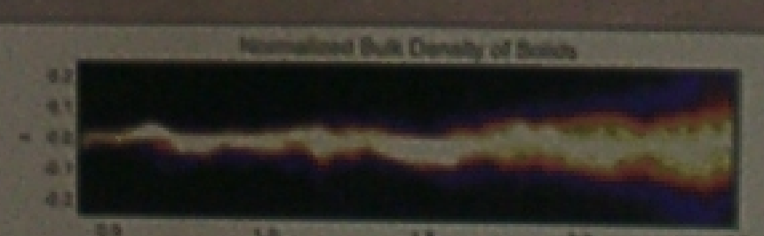

Vertical slice of the bulk density of solid particles normalized by the midplane density. A midplane layer forms in equilibrium between sedimentation and turbulent diffusion.

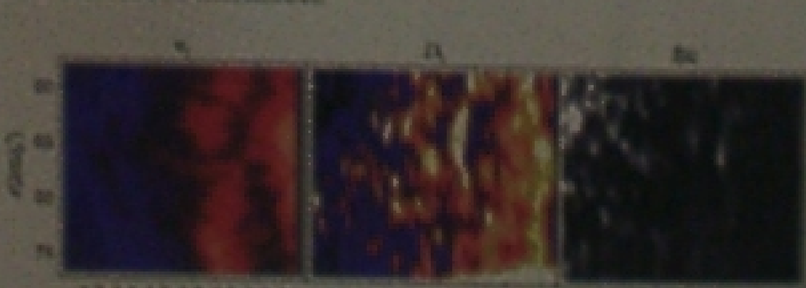

Azimuthally and vertically averaged turbulent viscosity ν_t, turbulent diffusion D_t and the resulting Schmidt number Sc as a function of radial position and time. Viscosity and diffusion are shown in the same units and color-code. Some localized overdensities in diffusion last for some orbits, while viscosity shows a smoother evolution in time. The quantities have approximately the same strength, as the Schmidt number is overall around unity, and seldom greater than 5.

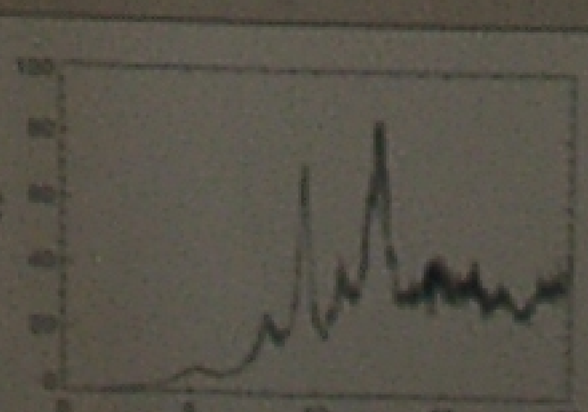

Maximum bulk density of solids, in units of the mean gas density as a function of time for model A. Time is quoted in orbits at s_0. The maximum density rises as the particles sediment towards the midplane. After the sedimentation that lasts for four orbits, the particles are coupled with the gas and trapping in transient gas high pressures raise their maximum density well above average. The maximum density is usually around 30, but between orbits 12 and 13, it reached values as high as 80.

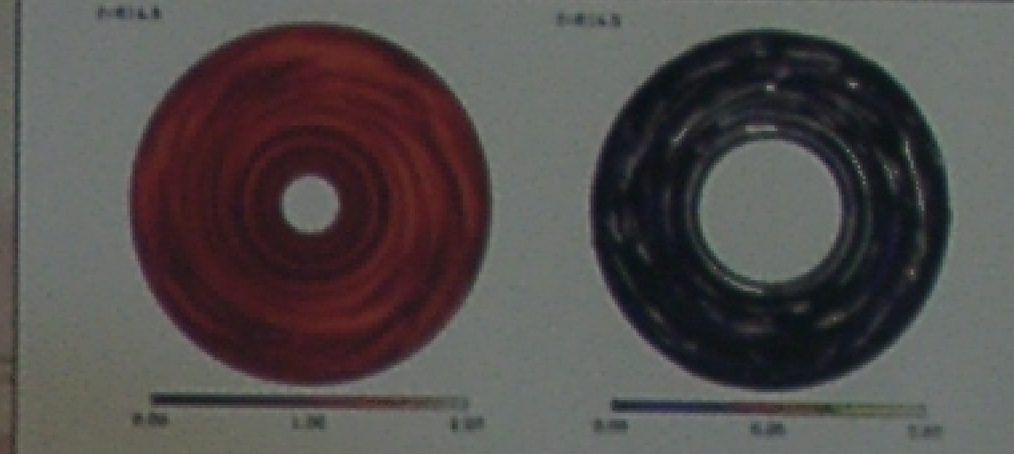

Density contours at midplane of the gas and solid phases of the disk (left and right panel, respectively) for model A. The snapshots were taken after 20 orbits at s_0 after the insertion of the particles. The color code for the solid phase is selected to represent 2 sigma (0.25) above the average bulk density of 0.03. The bright areas are saturated as the maximum density is order of magnitude greater. A correlation with gas density is seen, since the bright clumps of solids correspond to pressure maxima, i.e, areas of high gas density.

Results

The models ran and their respective outcomes are specified in the table below

Table 2. Cylindrical turbulent disk models.

Run	Parameters	Results
Uniform Field B_z		
A	[illegible]	[illegible]
B	[illegible]	[illegible]
C	[illegible]	[illegible]
A2	[illegible]	[illegible]
B2	[illegible]	[illegible]
C2	[illegible]	[illegible]
Radially Varying Field B_z		
D	[illegible]	[illegible]
E	[illegible]	[illegible]
Uniform Field B_ϕ		
F	[illegible]	[illegible]

The results are summarized as follows:

- The turbulence generated by the magnetorotational instability grows with the thermal pressure. The turbulent stresses depend on thermal pressure obeying a power law of 0.24 ± 0.03.
- The ratio of stresses $-M^{s\phi}/R^{s\phi}$ diminished with increasing temperature. It is 5 for model A, and just 1.3 for model C. It is 6.5 for model A2 and very close to 1 for model C2. This effect is unexpected since it is believed that the shear parameter alone controls the ratio of stresses.
- In treating the solids, we make use of a large number of particles, monitoring their settling toward the midplane and the formation of a sedimentary layer when the solids are subject to gas drag and the gravity from the central object. The effective diffusion provided by the turbulence prevents further settling. The measured scale heights imply turbulent vertical diffusion coefficients with globally averaged Schmidt numbers of 1.0±0.2 for model A ($\alpha \approx 10^{-3}$) and 0.78±0.06 for model D ($\alpha \approx 10^{-1}$).
- The average bulk density of the solids is quite low (ρ_p=0.003, or 6.0×10^{-14} g cm^{-3} in physical units, see Table 1 for conversion), but very dense clusters of solids are seen trapped in the high pressure regions of the turbulent flow. In these areas, the solids-to-gas ratio is raised by 4 orders of magnitude with respect to the initial condition. Such large concentrations are prone to become gravitationally bound, thus collapsing to form km-sized protoplanets.
- The next steps of the project can be summarized in:
  - Vertical stratification
  - Solving for neutrals as well as ions
  - Including self-gravity on both the gas and solids phase
  - Explicit ray tracing radiative transfer to yield observables (fluxes)
- Movies of the simulations can be found at http://www.astro.uu.se/~wlyra/planet.htm